ChemComm

Accepted Manuscript

This article can be cited before page numbers have been issued, to do this please use: Sk. A. Rahaman, D. K. Mondal and S. Bandyopadhyay, *Chem. Commun.*, 2019, DOI: 10.1039/C8CC10035G.

ROYAL SOCIETY OF CHEMISTRY

rsc.li/chemcomm

View Article Online
DOI: 10.1039/C8CC10035G

COMMUNICATION

Formation of disulphide linkages restricts intramolecular motions of fluorophore: Detection of molecular oxygen in food package

Sk. Atiur Rahaman, Dipon Kumar Mondal and Subhajit Bandyopadhyay*[a]

Received 00th January 20xx,
Accepted 00th January 20xx

DOI: 10.1039/x0xx00000x

www.rsc.org/

Reliable and easy detection of oxygen in food packaging without the aid of sophisticated instruments is highly coveted. A tetraphenylethene probe based on the oxygen mediated polymerization via the formation of disulfides causes restricted intramolecular rotation the TPE phenyls resulting in a >100 fold enhancement of emission and thus detects O_2 in food package.

Oxygen is one of the most important chemical species for life on earth. An adult human metabolizes ~200 g of oxygen per day. Determination of molecular oxygen has important implications for bio-medicinal,[1] industrial, and environmental chemistry.[2] As a consequence, several classes of luminescence-based oxygen sensors have been developed in the last few year.[3–8] Most of these probes make use of transition metal complexes immobilized in polymeric matrices as the active luminescent species.[9–11] Some luminescent porous coordination polymers (PCPs) have been recently reported as attractive oxygen-sensing materials.[12–16] Most of the luminescent based oxygen sensors function with a turn-off response in the presence of oxygen. Although, they can be useful for the detection of molecular oxygen, a turn-on response is perhaps more coveted as the fluorescence enhancement is more discernable to the naked eyes.

The shelf-life of a pre-packed food depends on oxygen as it promotes the growth of fungi and microorganisms. Most organisms could not survive the powerful oxidative properties of reactive oxygen species (ROS), highly unstable ions and molecules derived from partial reduction of oxygen that can damage virtually any macromolecule or structure with which they come in contact. Pathogenic bacterial species such as *Salmonella spp., Listeria monocytogenes, Staphylococcus aureus* and enteropathogenic *Escherichia coli* O157:H7 can pose high risk to the safety of meat and dairy products for the consumers. Aerobic strains of *Escherichia coli* can grow in packaged dairy product and meat in the presence of oxygen efficiently. Therefore products such as cheese and meat are specially packaged under nitrogen. Certain moulds can grow on a variety of food items including nuts, dried fruits, cereals and coffee beans in the presence of oxygen under warm and humid conditions. These fungi can produce naturally occurring toxins called the mycotoxins which can sometimes be lethal. Small leakages in the foodstuff packed under vacuum or nitrogen can sometimes allow oxygen to be present in the package which might reduce the shelf-life of the food. Each year there are instances of a number of recalls of the food products because of the presence of the contaminated strains of bacteria in packaged food products. Early detection of trace amount of oxygen in the packaged food can be indicative of the health of the packed food. Therefore, it is important to device a cheap, easy-to-use, stench-free, non-toxic and metal-free marker for the detection of oxygen for food packaging.

Here we report a metal free thiol appended tetraphenylethene (TPE) based system **1** that detects molecular oxygen with a large (>100 fold) enhancement of emission intensity. The probe exploits the simple chemistry where the thiol units readily form disulfide linkages and results in a restricted intramolecular rotation of the phenyl rings of the molecule. Moreover, the scanning electron microscopy (SEM), the advanced Polymer Chromatography (APC) and the dynamic light scattering (DLS) measurements were performed to confirm the formation of a

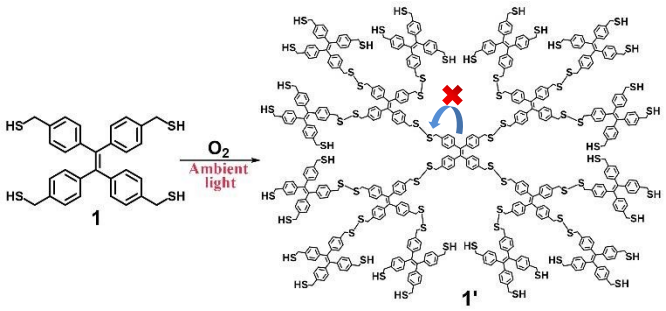

Fig. 1 Formation of a disulphide polymer of **1** upon areal oxidation and restricted intramolecular rotation of the phenyl rings.

[a] *Department of Chemical Sciences, Indian Institute of Science Education and Research (IISER) Kolkata, Mohanpur, Nadia, WB 741246 India*
[b] *Electronic Supplementary Information (ESI) available: Experimental section, additional figures and tables, SCXRD data. See DOI: 10.1039/x0xx00000x*

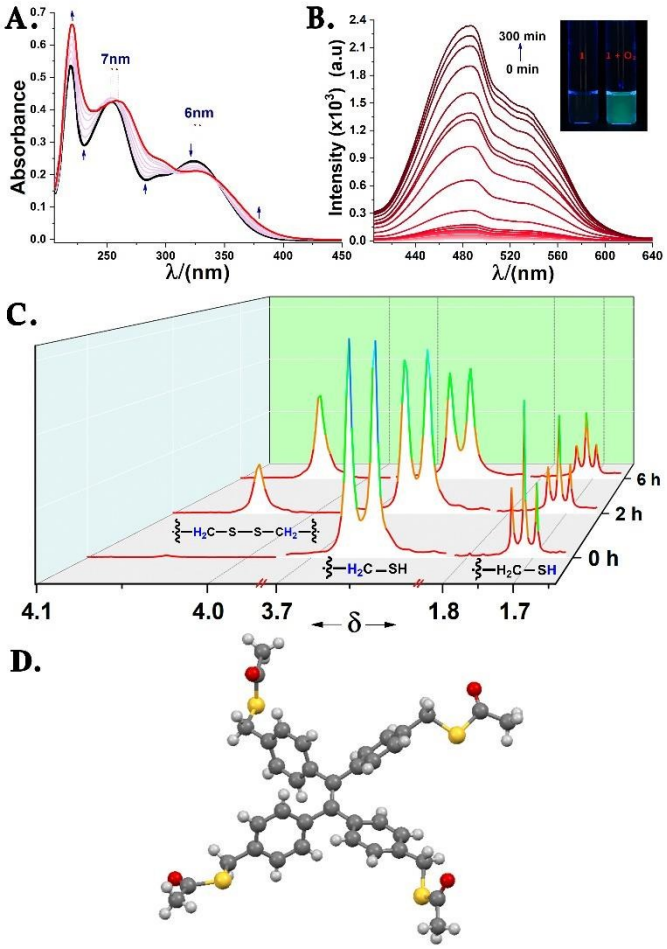

UV-vis absorption spectra of compound **1** (10 μM), (B) changes in the emission spectra of compound **1** (10 μM) (λ_{ex}: 320 nm, slit: 5/5); Inset: visual change under 366 nm light in THF media at 25 °C. (C) Time dependent changes in the ^{1}H NMR spectra of compound **1** (1 mM) in $CDCl_3$ at 25 °C upon bubbling with air, (D) SCXRD structures of compound **2**.

polymer upon introducing of oxygen in the THF solvent. This is different from the classical mechanism of aggregation-induced emission (AIE) effect,[17-18] where the enhancement in the emission signal is a result of the aggregation of the TPE species in an aqueous media, first reported by Tang *et al*.[19] Normally, TPE based supramolecular polymers exhibit higher emissions in the aggregated state compared to the non-aggregated monomeric forms due to the restricted rotation of the phenyl ring in the stacked states in the aqueous media.[20] Based on this principle they have been used as building block units in luminescent porous materials, such as metal–organic frameworks (MOFs), covalent organic frameworks (COFs), supramolecular organic frameworks (SOFs), hydrogen-bonded organic frameworks (HOFs) and porous polymers. [21-25]

Compound **1** was prepared via deacetylation of the TPE thioacetate **2** in an inert atmosphere and characterized by spectroscopic and mass spectrometric methods (see Supporting Information, Experimental details). The single crystal XRD structure of the acetyl protected probe **1**, i.e., compound **2** was obtained (CCDC Number 1879842, See Fig. 2D and ESI†). The photophysical properties of compound **1** were investigated by

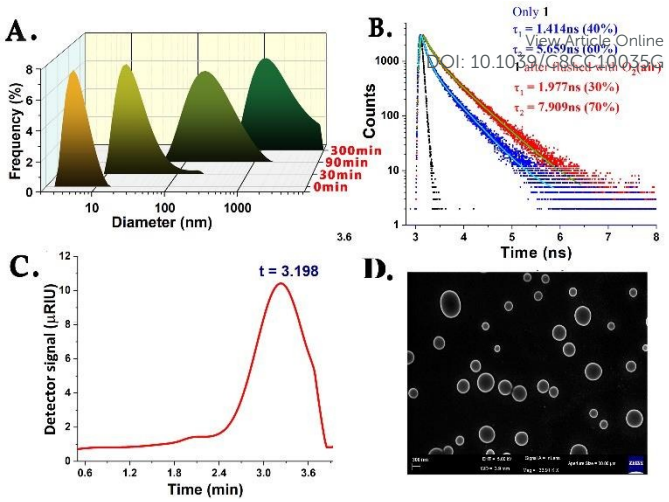

Fig. 3 (A) The particle size distribution monitored by DLS studies after the bubbling of O_2 to **1** (10 μM) in THF solvent at various time intervals, (B) TCSPC experiments displaying the decay times of **1** prior to and after bubbling with air (300 min) at 25 °C. (C) APC analysis of the **1'** polymer (10 μM), (D) SEM image of a dried sample of **1'**.

UV-vis spectroscopy and fluorescence spectroscopy in the THF media.

It is well known that in THF, the free rotation of the phenyl rings of the propeller-shaped TPE is responsible for the non-radiative energy dissipation from the excited state. However, in the presence of water, the hydrophobic TPE molecules aggregate restricting the rotation of the phenyl rings and also the nonradiative relaxation channel populating the radiative excitons, which confers the TPE units a strong emissive character. This phenomenon is popularly known as the aggregation induced emission (AIE).[26-27] Our thiol appended molecule containing the TPE luminogen shows a faint emission in THF solution. As expected, the emission increases drastically upon aggregation in the THF/water mixtures with higher fractions of water. At 95% water content, bright cyan emission is observed upon exposure under 366 nm UV light (see Fig. S6-S7, ESI†).

However, even in THF in the presence of oxygen, a large enhancement of the fluorescence was observed with the tetrathiol **1**. The enhancement of the emission in this case was way more than that observed for the AIE in the 95 % (v/v) water in THF. From the UV-vis spectroscopy in a THF solution, it was found (Fig. 2A) that the absorption of compound **1** at 324 nm decreased with a 6 nm red shift. The band at 253 nm displayed a 7 nm red shift upon the introduction of O_2 from air. The emission spectra of the aerated solution of **1** (10μM) displayed a remarkable 112 fold enhancement of the fluorescence intensity at 485 nm (Fig. 2B) (($\Phi = 0.17$) with a 5 nm red shift compared to the initial band of **1** ($\Phi = 0.0012$, compared to quinine sulfate)). The response of probe **1** at various partial pressures of O_2 is shown in figure S11. The LOD of O_2 detection was found to be 30.8 torr (Figure S15). The fluorescence change of compound **1** could be clearly observed with naked eyes under the 366 nm UV light as shown in the Fig. 2B (*insert*)). We envisaged that the tetrasulfide **1** in the presence of molecular oxygen in the presence of the ambient light led to the formation of the disulphide linkage (Fig. 1). The network of the disulphide

linkages stops the intramolecular rotation of phenyl rings in the polymeric **1'** and thereby converting it to a highly emissive species. Since it is known that thiols can be converted to disulfides with hydrogen peroxide or iodine,[28] it was envisaged that upon treatment of **1** with H_2O_2 or I_2, similar polymeric species could be generated that would display similar spectroscopic properties that was observed with **1** in the presence of oxygen. Thus, compound **1** (10 μM) was treated with separately with I_2 (10 μM) and H_2O_2 (10 μM) in THF. The emission spectra of samples of **1** after the treatment with iodine, and H_2O_2 displayed similar emission pattern and enhancement (see Fig. S8-S9, ESI†). However, the reaction with H_2O_2 reached a saturation of the emission intensity in less than 30 min. With I_2 the reaction required 2 h, and with O_2, the saturation of the emission intensity required bubbling for 5 h (see Fig. S9, ESI†).

To verify the mechanism, particle size analysis was performed by dynamic light scattering experiments. A solution of compound **1** in THF was found to possess a hydrodynamic radius of 4.7 nm perhaps from the small aggregates of the organic molecule. After bubbling the solution with gaseous oxygen for a period of 30 minutes with a bubbling rate of roughly one bubble per second, the hydrodynamic diameter was found to increase to 196.0 nm. The size dependence of the particles with the bubbling time was systematically studied by DLS in THF media at 25 °C. Upon the bubbling of the atmospheric air through a solution of **1**, the DLS experiment revealed that the particle size increased rapidly with time. After 300 minutes of bubbling the particle size displayed a saturation value with an average diameter of 1362.9 nm of the Z-average hydrodynamic diameter (Fig. 3A).

The fluorescence lifetimes of compound **1** before and after exposing to oxygen **(1')** was studied by TCSPC experiments in the THF. In both the cases, the decay profile followed a biexponential decay pattern Fig. 3B. The lifetimes and the relative amplitudes of the components are provided in Table 1. The average lifetime of fluorescence increases from 3.7 to 6.34 ns upon polymerization in the presence of oxygen. In addition, the component with the shorter lifetime (τ_1) decreases upon the polymerization, whereas the component for the longer lifetime (τ_2) increases. From the point of view of the molecular structure of compound **1** and polymer **1',** it is conceivable that the polymer has restricted intramolecular rotation of the phenyl rings which is responsible for its higher fluorescence lifetime.

Table 1 Fluorescence lifetimes for compound **1** and polymer **1'**

Compound	τ_1 (ns)	τ_2 (ns)	$\langle\tau\rangle$ (ns)	χ^2
1	1.41	5.659	3.703	1.15
1'	1.97 (± 0.)	7.909	6.362	1.13

To gain an insight of the changes in the molecular structure upon the exposure to oxygen, O_2 gas was bubbled through a sample of **1** in $CDCl_3$ solvent and the ^{1}H NMR spectra were recorded at various time intervals. With the increase in the bubbling time, the signal for the doublet methylene protons next to the –SH group at δ 3.67 decreased gradually and a new singlet peak at δ 4.03 which can be attributed to the $–CH_2$-S-S-

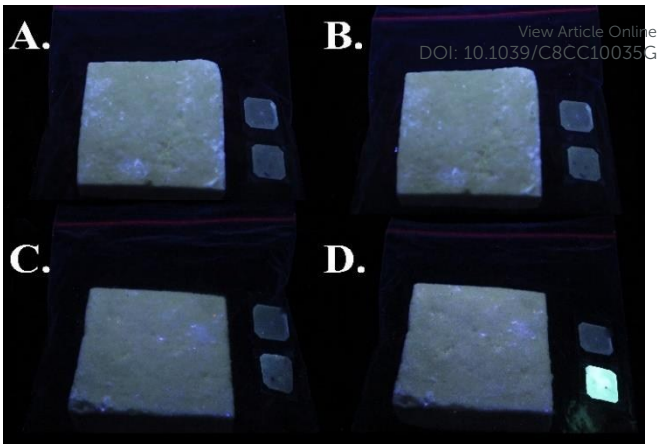

Fig. 4 Photographs of the cheese samples having two O_2-indicator strips, (the probe and the control) under 366 nm handheld light; (A) and (B) packed under N_2 t = 0 and 4 days respectively (C) and (D) packed under atmospheric air, t = 0 and 2 days respectively. Note the bright emission from the probe in panel (D).

CH_2- was observed (Fig. 2C). The decrease in intensity of the thiol protons were also apparent from the NMR integration values. The integration of the $–CH_2$- protons were calibrated against the aromatic protons. The ratio of the newly formed –C**H**$_2$-S-S- : C**H**$_2$SH protons obtained from the ^{1}H-NMR integrations was 0.85: 1 which is consistent with the expected structure of **1'** where this ratio is expected to be 0.88:1. There was also a concomitant decrease in the intensity of the –SH protons due to formation of **1'**. The changes in the signals of the other protons were small. The shift in the ^{13}C NMR signals (see Fig. S10, ESI†) were also quite prominent and has been summarized in Table S1. The decrease in the intensity of the thiol protons, the new methylene peaks and the shifts in the ^{13}C NMR clearly indicates the crosslinking of a number of the TPE units through the formation of –S–S– linkages. It is noteworthy that bubbling molecular oxygen through the NMR tube for > 7 h lead to the formation of an intractable sticky precipitate presumably due to the formation of larger polymeric structure. The average molecular weight (M_n) determined from the advanced polymer chromatographic (APC) studies was 8900 D with an index of polydispersity value of 1.2 at retention time with 3.198 min (see Fig. 3C). This clearly indicates the presence of an average of seventeen TPE units in the cross-linked polymer which is consistent with the ^{1}H-NMR data.

The SEM images of a dried sample of compound **1** and polymer **1'** from a THF solution were recorded (see Fig. S13, ESI† and Fig. 3D). The compound **1** shows irregular surface with the aggregated dry samples with an average size of 298 nm. The polymeric **1'**, on the other hand, displayed a rather spherical shape with an average size of 590 nm.

To check the reversibility of the probe and revalidate the mechanism, the disulphide **1'** was treated with a reducing agent, sodium borohydride. Upon systematic treatment of $NaBH_4$ in THF, the emission intensity of **1'** was found to diminish and finally reach a saturation value which was similar to the probe **1** because of the conversion of **1'** to **1** via the reduction of the –S-S- linkages to –SH (see Fig. S10, ESI†).

For practical application of compound **1** as a probe for the detection of the presence of oxygen in sealed food packages, two samples of cheese (paneer), one packed under nitrogen gas and the other under atmospheric air were used Indicator labels were prepared from Whatman 1 filter papers (2 cm x 2 cm) dipped in a solution of 10 mM of **1** in THF and subsequently air dried. It is to be noted that the paper strips did not have any malodour of sulphides presumably because of its low concentration and volatility. For each of the packed cheese, two indicator labels, one as an oxygen probe (Fig. 4C and 4D, bottom labels) and the other as a control (Fig 4A and 4B. top labels) were placed inside the sealed packages. The control labels were covered with transparent cellulose tape to avoid its exposure to air; the indicator probe was attached to the inner surface of the packaging plastic layer with a spot of household PVA glue. After two days, the indicator packed under air showed bright emission (Fig. 4D). However the control-indicator label in the package containing the cheese packed under nitrogen did not display any significant enhancement of the emission even after 4 days (Fig. 4B). However, lower amount of O_2 can be detected with the probe **1**, if it is exposure to O_2 over a longer period of time. Probe **1** thus offers an economically viable (<$0.05 or <£ 0.04 per indicator label) detection technique for oxygen in food packages. The probe is metal-free probe and the detection does not require any sophisticated instrument and is therefore promising for smart-packaging of vacuum or nitrogen packed convenient food.

Toxicity analysis by the MTT assay was studied with probe **1** against the mammalian cell line J774A.1. The viability of probe **1**-treated J774A.1 macrophage reveals that the probe did not have any significant toxicity on the cell viability upto $100\ \mu M$ (Figure S16).

In summary, in this work we have synthesized a tetrathiol appended TPE system that undergoes a polymerization via an oxidative transformation of the thiols to disulfides. This transformation causes a restriction the propeller-like rotation of the TPE-phenyl rings thereby causing a large enhancement of the emission of the AIEgen via a less conventional mechanism that does not involve aggregation of the TPE. The mechanism is operative in solution and even in paper test strips. Oxygen detection in packed samples carried out with the test strips coated with compound **1** demonstrated its potential use for food packaging.

SB acknowledges DST-SERB for a research grant (EMR/2017/003720) for the financial assistance. SAR is supported by a doctoral fellowship from IISER Kolkata.

Conflicts of interest

There are no conflicts to declare.

Notes and references

1 C. Prelnlnger, I. Kllmant, and O. S. Wolfbeis, *Anal. Chem.*, 1994, **66**, 1841-1846.
2 H. Li, J. Li, Z. Ai, F. Jia, and L. Zhang, *Angew. Chem. Int. Ed.*, 2018, **57**, 122 – 138.
3 (a) R. I. Dmitriev and D. B. Papkovsky, *Methods Appl. Fluoresc.*, 2015, **3**, 034001, (b) S. Sun, B. Ungerböck and T. Mayr, *Methods Appl. Fluoresc.*, 2015, **3**, 034002.
4 (a) P. W. Zach, O. T. Hofmann, I. Klimant, and S. M. Borisov, *Anal. Chem.*, 2018, **90**, 2741−2748. (b) Z. Sun, C. Cai, F. Guo, C. Ye, Y. Luo, S. Ye, J. Luo, F. Zhu, and C. Jiang, *Nanotechnology*, 2018, **29**, 145704.
5 J. An, C. M. Shade, D. A. Chengelis-Czegan, S. Petoud, and N. L. Rosi, *J. Am. Chem. Soc.*, 2011, **133**, 1220–1223.
6 M. Eltermann, V. Kiisk, A. Berholts, L. Dolgov, S. Lange, K. Utt, and R. Jaaniso, *Sensors and Actuators B*, 2018, **265**, 556–564.
7 Y. Zheng, Y. Jiao, Y. Zhu, Q. Cai, A. Vasileff, L. H. Li, Y. Han, Y. Chen, and S. –Z. Qiao, *J. Am. Chem. Soc.*, 2017, **139**, 3336−3339.
8 X. Chen, X. Tian, I. Shin, and J. Yoon, *Chem. Soc. Rev.*, 2011, **40**, 4783–4804.
9 K. Y. Zhang, P. Gao, G. Sun, T. Zhang, X. Li, S. Liu, Q. Zhao, K. K.-W. Lo, and W. Huang, *J. Am. Chem. Soc.*, 2018, **140**, 7827−7834.
10 P. Mani, A. Sheelam, S. Das, G. Wang, V. K. Ramani, K. Ramanujam, S. K. Pati, and S. Mandal, *ACS Omega*, 2018, **3**, 3830−3834.
11 R.-W. Huang, Y.-S. Wei, X.-Y. Dong, X.-H. Wu, C.-X. Du, S.-Q. Zang, and T. C. W. Mak, *Nat. Chem.*, 2017, **9**, 689–697.
12 N. Acha, C. Elosúa, I. R. Matías, and F. J. Arregui, *Sensors and Actuators B*, 2017, **248**, 836-847.
13 X. Jiang, J. Peng, J. Wang, X. Guo, D. Zhao, and Y. Ma, *ACS Appl. Mater. Interfaces*, 2016, **8**, 3591−3600.
14 J.-W. Ye, J.-M. Lin, Z.-W. Mo, C.-T. He, H.-L. Zhou, J.-P. Zhang, and X.-M. Chen, *Inorg. Chem*., 2017, **56**, 4238−4243.
15 F. Lin, F. Li, Z. Lai, Z. Cai, Y. Wang, O. S. Wolfbeis, and X. Chen, *ACS Appl. Mater. Interfaces*, 2018, **10**, 23335−23343.
16 X.-d. Wang and O. S. Wolfbeis, *Chem. Soc. Rev.*, 2014, **43**, 3666—3761.
17 Y. Wu, H. Hua and Q. Wang, *New J. Chem.*, 2018, **42**, 8320-8324.
18 Q. Zhaoa and Y. Liu, *Chem. Commun.,* 2018, 54, 6068—6071.
19 (a) J. Mei, Y. Hong, J. W. Y. Lam, A. Qin, Y. Tang and B. Z. Tang, *Adv. Mater*., 2014, **26**, 5429. (b) Y. Hong, J. W. Y. Lam and B. Z. Tang, *Chem. Soc. Rev*., 2011, **40**, 5561-5388. (c) C. Coluccini, A. K. Sharma, M. Caricato, A. Sironi, E. Cariati, S. Righetto, E. Tordin, C. Botta, A. Forni, D. Pasini. *Phys. Chem. Chem. Phys*., 2013, **15**, 1666—1674. (d) A. Nitti, F. V.-Monteleone, A. Pacini, C. Botta, T. Virgili, A. Forni, E. Cariati, M. Boiocchif, D. Pasini, *Faraday Discuss.*, 2017, **196**, 143–161.
20 J. Mei, N. L. C. Leung, R. T. K. Kwok, J. W. Y. Lam, and B. Z. Tang, *Chem. Rev.*, 2015, **115**, 11718–11940.
21 X.-G. Liu, H. Wang, B. Chen, Y. Zou, Z.-G. Gu, Z. Zhao and L. Shena, *Chem. Commun.*, 2015, **51**, 1677—1680.
22 N. Baroni, A. Turshatov, M. Adams, E. A. Dolgopolova, S. Schlisske, G. Hernandez-Sosa, C. Wöll, N. B. Shustova, B. S. Richards, and I. A. Howard, *ACS Appl. Mater. Interfaces*, 2018, **10**, 25754−25762.
23 Z. Zhou, X. Yan, M. L. Saha, M. Zhang, M. Wang, X. Li, and P. J. Stang, *J. Am. Chem. Soc.*, 2016, **138**, 13131−13134.
24 M. Zhang, G. Feng, Z. Song, Y.-P. Zhou, H.-Y. Chao, D. Yuan, T. T. Y. Tan, Z. Guo, Z. Hu, B. Z. Tang, B. Liu, and D. Zhao, *J. Am. Chem. Soc.*, 2014, **136**, 7241−7244.
25 N. B. Shustova, T.-C. Ong, A. F. Cozzolino, V. K. Michaelis, R. G. Griffin, and M. Dinca, *J. Am. Chem. Soc.*, 2012, **134**, 15061−15070.
26 R. Hu, N. L. C. Leungb and B. Z. Tang, *Chem. Soc. Rev.*, 2014, **43**, 4494—4562.
27 D. D. La, S. V. Bhosale, L. A. Jones, and S. V. Bhosale, *ACS Appl. Mater. Interfaces,* 2018, **10**, 12189−12216.
28 M. Kirihara, Y. Asai, S. Ogawa, T. Noguchi, A. Hatano, Y. Hirai, *Synthesis*, 2007, **21**, 3286-3289.

